

# Plasmonic nanorod metamaterials for nanochemistry and sensing

*Pan Wang<sup>1,2,\*</sup>, Mazhar E. Nasir<sup>1</sup>, Alexey V. Krasavin<sup>1</sup>, Wayne Dickson<sup>1</sup>, Yunlu Jiang<sup>1</sup>, and Anatoly V. Zayats<sup>1,\*</sup>*

<sup>1</sup>Department of Physics and London Centre for Nanotechnology, King's College London, Strand, London WC2R 2LS, UK

<sup>2</sup>State Key Laboratory of Modern Optical Instrumentation, College of Optical Science and Engineering, Zhejiang University, Hangzhou 310027, China

CONSPECTUS: Plasmonic nanostructures have initially been developed for sensing and nanophotonic applications but recently shown great promise in chemistry, opto-electronics and nonlinear optics. While smooth plasmonic films, supporting surface plasmon polaritons, and individual nanostructures, featuring localized surface plasmons, are easy to fabricate and use, the assemblies of nanostructures in optical antennas and metamaterials provide many additional advantages related to the engineering of the mode structure (and thus, optical resonances in the given spectral range), field enhancement and local density of optical states required to control electronic and photonic interactions. Focusing on two of the many applications of plasmonic metamaterials, in this Account we review our work on sensing and nanochemistry applications of metamaterials based on the assemblies of plasmonic nanorods under optical as well as electronic

interrogation. Sensors are widely employed in modern technology for the detection of events or changes in their local environment. Compared to their electronic counterparts, optical sensors offer a combination of high sensitivity, fast response, immunity to electromagnetic interference, as well as providing additional options for signal retrieval, such as optical intensity, spectrum, phase, and polarization. Owing to the ability to confine and enhance electromagnetic fields on subwavelength scales, plasmonics has been attracting increasing attention for the development of optical sensors with advantages including both nanometer-scale spatial resolution and single-molecule sensitivity. Inherent hot-electron generation in plasmonic nanostructures under illumination or during electron tunneling in the electrically biased nanostructures provides further opportunities for sensing and stimulation of chemical reactions which would otherwise not be energetically possible.

We first provide a brief introduction to a metamaterial sensing platform based on arrays of strongly coupled plasmonic nanorods. Several prototypical sensing examples based on this versatile metamaterial platform are presented. Record-high refractive index sensitivity of gold nanorod arrays in biosensing based on the functionalization of the nanorod surface for selective absorption arises due to the modification of the electromagnetic coupling between the nanorods in the array. The capabilities of nanorod metamaterials for ultrasound and hydrogen sensing were demonstrated by precision coating of the nanorods with functional materials to create core-shell nanostructures. The extension of this metamaterial platform to nanotube and nanocavity arrays, and metaparticles provides additional flexibility and removes restrictions on the illumination configurations for the optical interrogation.

We then discuss a nanochemical platform based on the electrically-driven metamaterials to stimulate and detect chemical reactions in the tunnel junctions constructed with the nanorods by exploiting elastic tunneling for the activation of chemical reactions via generated hot-electrons and

inelastic tunneling for the excitation of plasmons facilitating optical monitoring of the process. This represents a new paradigm merging electronics, plasmonics, photonics and chemistry at the nanoscale, and creating opportunities for a variety of practical applications, such as hot-electron-driven nanoreactors, high-sensitivity sensors as well as nanoscale light sources and modulators. With a combination of merits such as the ability to simultaneously support both localized and propagating modes, nanoporous texture, rapid and facile functionalization and low cost and scalability, plasmonic nanorod metamaterials provide an attractive and versatile platform for the development of optical sensors and nanochemical platforms using hot-electrons with high performance for applications in fundamental research and chemical and pharmaceutical industries.

## 1. INTRODUCTION

Surface plasmons are the collective oscillations of free carriers near interfaces, which manifest in the form of surface plasmon polaritons (SPPs), surface electromagnetic waves propagating at an interface between a conductor and a dielectric, or as localized surface plasmons (LSPs) in the confined geometries<sup>1,2</sup>. Plasmonics has initially emerged for controlling optical signals at the subwavelength scales and rapidly expanded to encompass sensing, opto-electronics, nonlinear optics, nanochemistry and nanomedicine.<sup>3-10</sup> This expansion is fueled by the unique intrinsic properties offered by plasmonic structures to concentrate electromagnetic fields on the subwavelength scales and the related strong local-field enhancement, resulting in the enhanced light-matter interactions.<sup>1,2</sup> By harvesting hot carriers generated from the non-radiative decay of surface plasmons which had long been considered purely detrimental to the plasmonic performance, groundbreaking applications in photocatalysis and photodetection have been demonstrated.<sup>9-11</sup> In a parallel development, plasmonic metamaterials and metasurfaces, consisting

of strongly interacting plasmonic nanostructures, have been realised to further enable control of the collective plasmonic resonances and field enhancement.<sup>12</sup>

Due to the strong confinement and enhancement of light at the interfaces of metallic structures, surface plasmons are extremely sensitive to changes in dielectric environment in nanoscale regions near the interface, which can be exploited for optical sensing applications. Since the first demonstration using surface plasmons for probing electrochemical interfaces<sup>13</sup> and the detection of gases,<sup>14</sup> chemical and biological sensing has become an important application area of plasmonics. Several types of plasmonic sensors based on resonant excitation of either SPPs<sup>4</sup> or LSPs<sup>15</sup> have been developed, detecting the refractive index (RI) changes of the surroundings or the enhanced Raman scattering signals.<sup>16</sup> In addition to environmental sensing, these plasmonic sensors are important in chemical, biochemical and pharmaceutical industries.

In the case of RI sensing, SPP-based sensors provide an extremely high detection sensitivity approaching  $10^{-7}$  RI units (RIU)<sup>4,17</sup>, but due to the relatively weak one-dimensional confinement of the electromagnetic field on metal films, they are less sensitive to analytes with a small molecular weight (normally, <500 Da), making it problematic for modern nanoscale (bio)chemical applications. In contrast, taking advantage of the stronger two or three dimensional confinement of electromagnetic radiation in metal nanostructures, LSP-based sensors are more suitable for the detection of small molecules.<sup>18</sup> Their overall RI sensitivity is, however, at least one order of magnitude smaller than that for SPP-based ones, typically not exceeding 100-400 nm/RIU.<sup>18,19</sup> Nevertheless, for plasmonic hot-carrier generation and applications in nanochemistry, LSP-based effects are more advantageous providing hot-carriers near the interfaces. The nanostructures also facilitate extraction of carriers to the immediate surroundings due to the relaxation of the momentum conservation via scattering on nanoscale features.<sup>20,21</sup>

Advances in chemistry and nanofabrication have led to a quest for the synthesis of plasmonic nanostructures of different shapes<sup>22</sup> in order to control spectral range of plasmonic resonances and field localization and enhancement in order to improve sensing and hot-carrier chemistry performance. There is, however, another route, which employs plasmonic metamaterials in order to achieve the same, utilizing large-scale plasmonic nanostructured arrays based on assemblies of nanorods, nanotubes, nanoholes, split-ring resonators and other nanostructures<sup>12,23–26</sup>. Among them, plasmonic nanorod metamaterials<sup>23–25</sup>, composed of arrays of aligned, strongly interacting plasmonic nanorods are especially beneficial for sensing and nanochemistry applications. They combine the nanoporous texture with large surface area and the ability to simultaneously support both localized and propagating plasmonic modes, thus enabling optical sensing merging advantages of both LSP and SPP-based sensors and achieving nanochemical reactors where hot-electron effects can be fully exploited. These strongly anisotropic metamaterials may exhibit hyperbolic dispersion, enabling a plethora of nanophotonic applications, ranging from waveguiding and imaging beyond the diffraction limit<sup>27,28</sup> to the enhancement of nonlinear optical effects<sup>29,30</sup> and fluorescence.<sup>31</sup>

In this Account, we will review the application of plasmonic nanorod metamaterials in both sensing and nanochemistry. We will first briefly introduce structural and optical properties of the metamaterials. Their performance in RI sensing applications for biochemical, gas and ultrasound sensing will be overviewed. Optical sensors based on other plasmonic metamaterial platforms such as nanotube and nanocavity arrays as well as plasmonic metaparticles will be also discussed. Finally, we will review a new nanochemical and sensing configuration based on hot-electron-induced chemical transformations in the electrically-driven metamaterials.

## 2. STRUCTURAL AND OPTICAL PROPERTIES

The nanorod metamaterial consists of a periodic array of metallic nanorods oriented perpendicular to a substrate and can be embedded in a matrix or exposed to surroundings (Figure 1A). They are fabricated by electrodeposition of metal into porous anodized aluminum oxide (AAO) templates.<sup>23-25</sup> Glass or silicon substrate can be used with a thin layer of gold (5–10 nm) for technological reasons. A layer of aluminium is then deposited such that following electrochemical anodization, the aluminum layer forms porous alumina. The diameter and separation of the nanorods are determined by the geometry of the AAO template (regulated by the conditions of anodization, typically in the range of 15–65 nm and 50–120 nm, respectively), while the length of the nanorods is controlled by the electrodeposition time (typically in the range 150–1200 nm) and, as an upper bound, the thickness of the AAO template. Benefitting from the scalable electrochemical fabrication technique, such metamaterials can cover macroscopic (centimeters squared) areas with a typical nanorod areal densities as high as  $10^{10}$ - $10^{11}$  cm<sup>-2</sup> (Figure 1B and 1C).

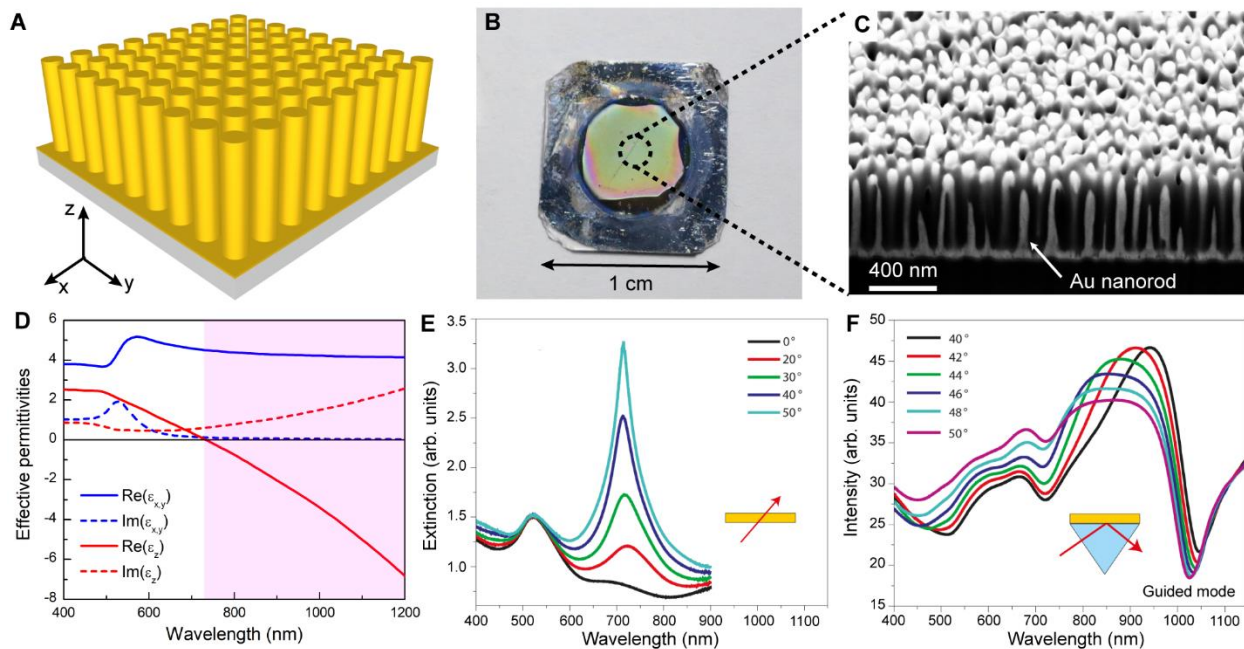


**Figure 1.** Structural and optical properties of nanorod metamaterials. (A) Schematic of the plasmonic nanorod metamaterial. The orientation of the Cartesian co-ordinates is also shown. (B) Photograph of a nanorod metamaterial chip. (C) Cross-sectional view of the metamaterial in B. Note that the apparent variations in the nanorods are due to the cross-section position. Reproduced with permission from ref 26. Copyright 2018 Nature Publishing Group. (D) Components of the effective permittivity tensor for a gold nanorod metamaterial ( $d = 25$  nm,  $s = 60$  nm). The coloured area shows the hyperbolic dispersion regime. (E, F) Extinction (E) and reflection (F) spectra of a gold nanorod metamaterial ( $d \approx 25$  nm,  $s \approx 60$  nm,  $l \approx 380$  nm) obtained in the transmission and ATR geometries, respectively, for various angles of incidence of the TM-polarized illumination. Reproduced with permission from Ref. 37. Copyright 2009 Nature Publishing Group.

Usually, the nanorod period is much smaller than the light wavelength, so that in the absence of diffractive effects, light perceives the nanorod array as a uniform medium. The anisotropic

optical response of the nanorod metamaterial can be described within the effective medium theory (EMT) by a diagonal permittivity tensor. The nonzero components of the tensor  $\varepsilon_x^{eff} = \varepsilon_y^{eff} \neq \varepsilon_z^{eff}$  can be expressed in the Maxwell-Garnet approximation<sup>32</sup> as

$$\varepsilon_{x,y}^{eff} = \frac{(1+p)\varepsilon_m + (1-p)\varepsilon_h}{(1-p)\varepsilon_m + (1+p)\varepsilon_h}, \quad (1)$$

$$\varepsilon_z^{eff} = p\varepsilon_m + (1-p)\varepsilon_h, \quad (2)$$

where  $p = \pi(d/2s)^2$  is the nanorod concentration, with  $d$  being the nanorod diameter and  $s$  being the period of the square lattice,  $\varepsilon_m$  and  $\varepsilon_h$  are the permittivities of the metal and the surroundings, respectively. Depending on the geometrical parameters of the metamaterial and the wavelength range, either elliptical ( $\text{Re}(\varepsilon_{x,y}^{eff}) > 0$ ,  $\text{Re}(\varepsilon_z^{eff}) > 0$ ) or hyperbolic ( $\text{Re}(\varepsilon_{x,y}^{eff}) > 0$ ,  $\text{Re}(\varepsilon_z^{eff}) < 0$ ) dispersion of the electromagnetic modes in the metamaterial can be observed (Figure 1D). It should be noted that this EMT description should be replaced with the nonlocal EMT theory<sup>33</sup> in certain cases when losses are low or when the local fields between the nanorods are important as in the case of nonlinear optical properties or emitters inside the metamaterial.

The optical properties of the metamaterial are determined by strong near-field coupling between plasmonic nanorods in the assembly.<sup>7,28,34–36</sup> The extinction spectra of a nanorod metamaterial obtained in the direct-transmission geometry with transverse magnetic (TM) polarized light exhibit two pronounced resonance peaks (Figure 1E).<sup>35–37</sup> The short-wavelength peak is associated with the light polarized perpendicularly to the nanorods (along the short axis). The long-wavelength peak with a strong angle of incidence dependence, which is observed for the light polarized along the long nanorod axis, is observed in the so-called epsilon-near-zero regime, around the effective plasma frequency of the metamaterial when  $\text{Re}[\varepsilon_z^{eff}(\omega)] = 0$ .<sup>28,33</sup> In the microscopic description, these extinction resonances are related to strongly interacting cylindrical

surface plasmons on the nanorods in the array.<sup>7</sup> The illumination of the same nanorod metamaterial in the attenuated total internal reflection (ATR) configuration reveals the structure of the guided modes of the metamaterial layer (Figure 1F).<sup>28,37</sup> By controlling the parameters of the metamaterial such as the diameter and length of and spacing between the nanorods, the optical properties can be tuned throughout the visible and near-infrared spectral range.<sup>38</sup>

### 3. REFRACTIVE INDEX SENSITIVITY AND BIOSENSING

The optical response (e.g., extinction and reflection spectra) of a plasmonic nanorod metamaterial, described by EMT, is determined not only by the plasmonic response of individual nanorods in the metamaterial, but also by the electromagnetic coupling between them. As a result, the optical response is sensitive to variations in the dielectric environment surrounding the nanorods as well as the coupling strength between the nanorods, which can be related to either a RI variation of the dielectric between them, or, in the case of mechanical stimuli, a change in the separation of the nanorods comprising the metamaterial (Eq. 1 and 2). For these reasons, plasmonic nanorod metamaterials have a great potential for sensing applications under oblique illumination when the modes with the field along the nanorods are measured under TM-polarized illumination.

The performance of a nanorod metamaterial for sensing applications was evaluated for both transmission and reflection configurations (Figure 2A) showing that indeed the analyte access between the nanorods is instrumental for the increased (~200-fold compared to its presence only on top of the metamaterial) sensitivity of both the spectral position of resonance peaks and the detected intensity.<sup>39</sup> The RI sensitivity increases for higher-order modes of the metamaterial sensor (Figure 2B) and with decreasing metamaterial thickness (Figure 2C). The requirements of the oblique illumination and TM-polarized light, essential for sensing with the nanorod-based

metamaterials, are removed for the nanotube arrays, where high sensitivity plasmonic modes of the nanotubes can be excited even at normal incidence.<sup>40</sup>

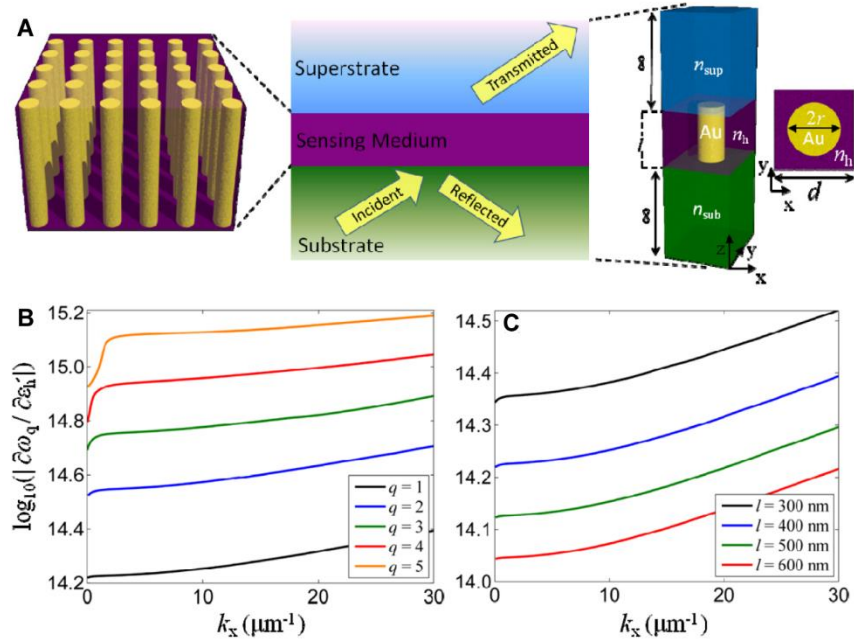


**Figure 2.** Sensing capabilities of the nanorod metamaterial slab. (A) Schematic of an array of gold nanorods for RI sensing experiments in the reflection or transmission geometry. (B, C) The mode frequency shift with variations of the real part of the analyte permittivity  $\varepsilon'_h$ : (B) the first five modes of the metamaterial slab for  $l = 400$  nm and (C) the fundamental mode ( $q = 1$ ) for various thicknesses of the metamaterial slab. Reproduced with permission from ref 39. Copyright 2015 Optical Society of American.

By incorporating a gold nanorod metamaterial illuminated in the ATR geometry in a flow cell (Figure 3A), the RI sensitivity of plasmonic resonances of the metamaterial was experimentally investigated.<sup>37</sup> The electromagnetic field of the guided modes (Figure 3B) is largely concentrated within the metamaterial slab. Therefore, the presence of the analyte molecules in the buffer surrounding the nanorods resulted in a RI sensitivity of  $\sim 32,000$  nm/RIU (Figure 3C and 3D), which is two orders of magnitude higher than the sensitivity of LSP-based sensors<sup>18,19</sup>

and until now is the record-high bulk RI sensitivity. The figure of merit ( $\text{FoM} = (\Delta\lambda/\delta\lambda)/\Delta n$ , where  $\Delta\lambda$  is the shift of a resonance peak to a RI change of  $\Delta n$ , and  $\delta\lambda$  is the full-width at half maximum of the resonance) of the nanorod metamaterial-based sensor reached a value of 330, which is much higher than that of LSP and SPP-based sensors.<sup>4,17-19</sup>

Using the well-established gold surface functionalization techniques,<sup>41</sup> the nanorod metamaterials can be tailored for specific analyte detection by functionalizing the nanorod surface with different kinds of biorecognition elements, e.g. antibodies. For example, by immobilizing a streptavidin-complex on the gold nanorod surface as a receptor (Figure 3E), the detection of a small molecular weight (244 Da) biotin molecules was demonstrated<sup>47</sup> with the detection limit more than two orders of magnitude better than that of conventional SPP-based sensors using continuous Au films.<sup>4,17</sup>

The requirements on the analyte volume can be reduced using shelled nanorods.<sup>37,42</sup> Generally, the alumina matrix protects nanorods and the field of the waveguided modes inside the metamaterial slab from the influence of the surrounding medium (Figure 1C), greatly limiting the sensing performance of nanorod metamaterials. When all the matrix is removed, significant amount of the analyte is needed to fill the space between the nanorods. The latter can be to some degree alleviated by the nanorod functionalization so that only molecules attached to the nanorods are detected. Additionally, there is a possibility to significantly reduce the sensed volume by creating, via chemical etching, an air-shell between the AAO matrix and the nanorods, which can produce zepto-litre sensing volumes.<sup>42</sup> Both transmission and ATR sensing configurations show high sensitivity of the resulting transducers.<sup>37,42</sup>

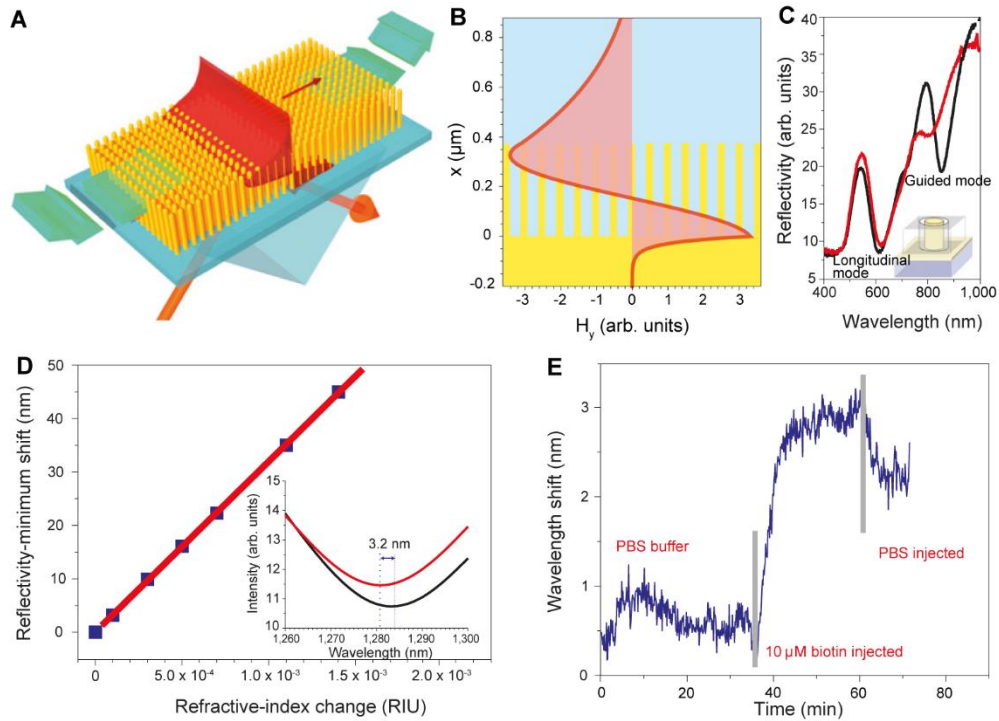


**Figure 3.** Biosensing with gold nanorod metamaterials. (A) Schematic of the ATR measurements in the flow cell configuration. (B) Calculated electromagnetic-field distribution of the guided mode in the metamaterial layer. (C) ATR spectra of a nanorod array with a 2 nm air-shell around the nanorods with different superstrates: (black) air and (red) ethanol. (D) Calibration curve for the metamaterial-based sensor (monitored at the reflectivity-minimum wavelength of 1230 nm) under step-like changes of the RI of the environment. Inset: Reflectivity spectrum modifications with  $\Delta n=10^{-4}$ . (E) Response of the metamaterial-based biosensor to the reaction of biotin-streptavidin binding. Reproduced with permission from ref 37. Copyright 2009 Nature Publishing Group.

#### 4. METAMATERIAL-ENHANCED RAMAN SPECTROSCOPY

Raman spectroscopy provides a spectral fingerprint of molecules and is an important analytical technique. Due to the small cross section of the Raman scattering, in many cases surface-enhanced Raman scattering (SERS) with nanostructured plasmonic substrates is used to amplify Raman signal by many orders of magnitude<sup>16,43</sup>. Different from the detection of specific analytes by surface functionalization discussed above, molecular detection based on SERS is label free.

The excitation of surface plasmons generates significantly enhanced electromagnetic fields in plasmonic nanorod metamaterials, making them a promising platform as substrates for enhancing Raman scattering. Using an array of silver nanorods, the strong dependence of SERS signal on the metamaterial geometry was demonstrated,<sup>44</sup> showing an over 200-fold SERS intensity increase by varying the interrod gap distance from 35 to 10 nm. This is due to the increasing electromagnetic fields in the gaps between neighboring nanorods with decreasing interrod gap distance.<sup>36,45</sup> This recipe is, however, limited to the distances of about 1 nm when the electron tunneling between plasmonic objects takes place and the field enhancement deteriorates.<sup>46</sup>

By creating gold nanorod arrays composed of two-segment dimer nanorods or coaxial nanorods with ~1 nm gap, the SERS signal of molecules self-assembled in the gap was additionally enhanced for ~30 times compared with the one-segment nanorod arrays case,<sup>47</sup> again due to the enhanced electromagnetic fields in the gaps. Recently, metamaterials based on gold nanocone arrays were fabricated, in which the electromagnetic fields are strongly confined in the ultra-sharp cone apex ( $\leq 5$  nm), representing a new structure for SERS applications.<sup>48</sup>

#### 5. CORE-SHELL NANOROD METAMATERIALS

The applications of the metamaterial sensing transducers can be extended by coating the surface of plasmonic nanorods with functional materials. Such core-shell nanorod metamaterials can be

readily fabricated by firstly widening the AAO pores to create a nanometric shell around the nanorods followed by the electrodeposition of the functional materials, such as palladium,<sup>49</sup> polypyrrole (PPy),<sup>50</sup> nickel<sup>51</sup> into the shells, to coat the nanorods.

### 5.1 Hydrogen Sensing

Hydrogen detection schemes generally present a trade-off between sensitivity and response time but safety is also important. Conventional hydrogen sensors are based on electric resistance changes and often operated at high temperatures<sup>52-54</sup>, therefore, increasing the explosive hazard. The elimination of electric currents in optical hydrogen sensors minimizes the risks. For the sensing of hydrogen gas, the nanorods forming the metamaterial were coated with a shell of palladium, which can undergo a reversible chemical transition from metal to metal hydride in the presence of hydrogen. The resulting Au-Pd core-shell nanorod array, after the removal of the alumina matrix to ensure the access of the hydrogen to the palladium shell, showed a ~40% change in the transmission,<sup>49</sup> which was clearly noticeable to the naked eye as a change in the brightness of light transmitted by the metamaterial (Figure 4A). Similarly, in the reflection geometry, a ~30% change in the reflectivity and a spectral shift of the resonant peak of ~30 nm was observed in the presence of hydrogen gas (Figure 4B). This hybrid Au-Pd based plasmonic sensor has several advantages in terms of sensitivity, low fabrication cost and easy optical readout over other optical hydrogen sensors based on a variety of structures such as Pd disks, Pd gratings on gold film, gold antenna coupled Pd disks.<sup>55</sup> The high sensitivity of this sensor to hydrogen results from a combination of both the change of the plasmonic properties of individual core-shell nanorods and the modification of inter-rod coupling in the metamaterial due to the refractive index and thickness changes of the palladium shell, respectively, both affecting the optical properties of the metamaterial. The sensor can be rapidly reset (< 2 s) by heating under the illumination with a laser

light.<sup>49</sup> The operating wavelength and the thickness of Pd shell can further be optimized to maximize the sensitivity and response time.

## 5.2 Ultrasound Sensing

The core-shell configuration can be functionalized with a polymer shell, which changes its RI under pressure induced by acoustic waves. Many polymers can be used to obtain such a coating using electro-polymerisation.<sup>56</sup> In this way, the optical detection of ultrasound and photoacoustic signals with high performance was demonstrated.<sup>50</sup>

Upon exposure to the pressure of an ultrasound pulse, the reflection from the metamaterial slab changes on the time scale of few hundred picoseconds, with the transient signal rise time of about 250 ps and complete recovery after 1 ns (Figure 4C). The responses of different Au-core/polymer-shell nanorod metamaterials to the induced pressure in the range of 5-500 kPa give a similar linear signal-pressure dependence (Figure 4D) and show more than one order of magnitude higher sensitivity compared to a gold-film based SPP sensor with the same polymer coating. The pressure detection limit is estimated to be approximately 500 Pa, which is at least an order of magnitude better than for the SPP-based ultrasound sensors operating in resonant conditions and commercially available high-frequency ultrasound transducers based on piezoelements.<sup>57</sup> Greater sensitivity (tens of Pa) to ultrasound pressure can be obtained using resonant optical systems with high Q-factors, e.g., ring-resonator structures.<sup>58</sup> They however have limitations on the bandwidth due to the finite circulation time of light in the resonators and high Q-factors restrict their dynamic range. The non-resonant nature, signal linearity, and sub-nanosecond response time (~GHz bandwidth) make the metamaterial-based ultrasound transducers very promising for health and biomedical applications.

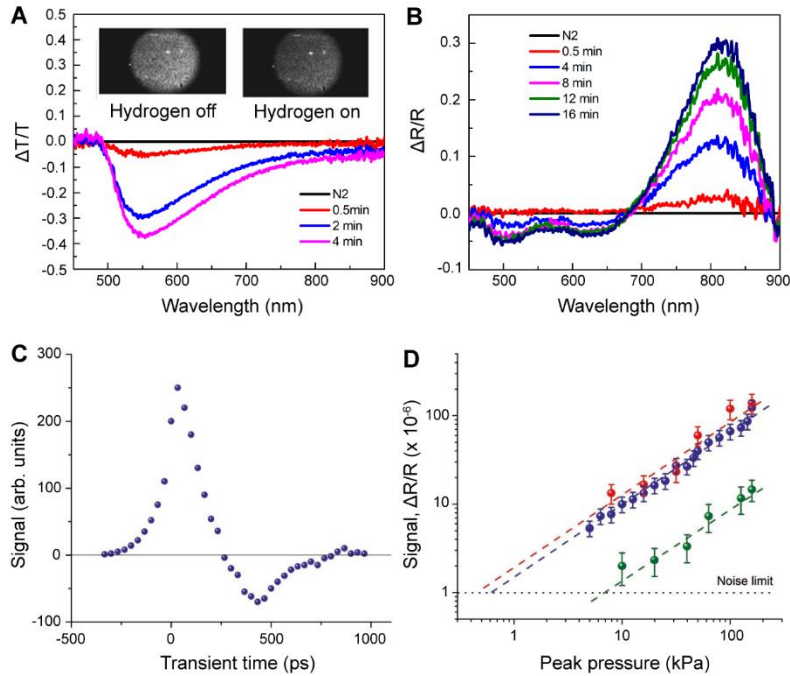


**Figure 4.** Optical sensors based on core-shell nanorod metamaterials. (A) Variation of transmission ( $\sim 40^\circ$  angle of incidence) of an Au-Pd core-shell nanorod metamaterial ( $l \approx 195$  nm) on exposure to 2%  $H_2$ . Inset: Photographs of the sensor in the absence and presence of  $H_2$ . (B) Variation of reflection ( $\sim 50^\circ$  angle of incidence) of an Au-Pd core-shell nanorod metamaterial ( $l \approx 280$  nm) to 2%  $H_2$ . (A, B) Reproduced with permission from ref 49. Copyright 2014 Wiley. (C) Transient response of an Au-PPy core-shell nanorod metamaterial upon arrival of an acoustic pulse at  $t=0$  ps. (D) The signal dependence on the acoustic pressure for the metamaterial sensors (red and blue) and the reference gold film-based SPP sensor (green). (C, D) Reproduced with permission from ref 50. Copyright 2013 Wiley.

## 6. ALTERNATIVE PLASMONIC METAMATERIALS FOR OPTICAL SENSING

In addition to the optical sensing platforms based on gold nanorod metamaterials and their core-shell counterparts, other variations of plasmonic metamaterials are important and useful for sensing and nanochemistry applications.

Gold nanotube metamaterials can be fabricated by electrodeposition of gold around sacrificial polymer nanorods in a porous AAO template<sup>23,40,56,59</sup> (Figure 5A). In contrast to the nanorod metamaterials which require oblique illumination with TM polarized light, the plasmonic resonances of nanotube metamaterials can be excited at normal incidence and are highly sensitive to RI of surroundings when both the inside and outside walls exposed to the analyte, showing a sensitivity of  $\sim 225$  nm/RIU (Figure 5B).<sup>40</sup> This can be understood from the electromagnetic field distribution of a free-standing nanotube array revealing the higher field enhancement along the outer tube wall than the inner wall, while near the rim of the nanotube the field is significant both inside and outside the tube (Figure 5C).

To further increase the field enhancement for higher sensitivity, coaxial rod-in-a-tube arrays were realized by the sequential deposition of gold nanorods, sacrificial PPy nanoshells, and gold nanoshells into porous AAO templates (Figure 5D).<sup>60</sup> By controlling the thickness of the sacrificial PPy nanoshells, the gap of the rod-in-a tube cavities can be made as small as 5 nm, resulting in a strong hybridization of the lowest order transverse dipolar modes of the nanorod and nanotube, and producing bonding and antibonding modes with strong field enhancement (Figures 5E and 5F). A sensitivity of  $\sim 400$  nm/RIU was predicted for the bonding modes, with the cavity being the most sensitive part of the structure (Figure 5G) and alone showing a bulk sensitivity of  $\sim 300$  nm/RIU compared to  $\sim 120$  nm/RIU for the outer walls only. The sensing performance of gold nanotube and coaxial nanocavity metamaterials can be further improved by exciting at oblique incidence.<sup>39</sup>

In addition to substrate-supported plasmonic metamaterials, a colloidal version of hyperbolic metamaterials (metaparticles) can be realized by coating gold nanospheres with alternating silica and gold forming multishell particles (Figure 5H).<sup>61</sup> These metaparticles possess a rich plasmonic mode structure including dipolar and quadrupolar resonances of various orders, which cover a broad wavelength range from 400 to 2200 nm (Figure 5I). Compared with gold nanospheres or nanoshells,<sup>18,19</sup> the metaparticles show greatly improved RI sensitivity, reaching a value as high as 740 nm/RIU, which is attractive for optical sensing applications with high flexibility and a broad spectral range. In addition, the strong and spectrally broad local-field enhancement in the metaparticles (Figure 5J) also makes them very useful for applications such as surface-enhanced Raman and infrared spectroscopies.

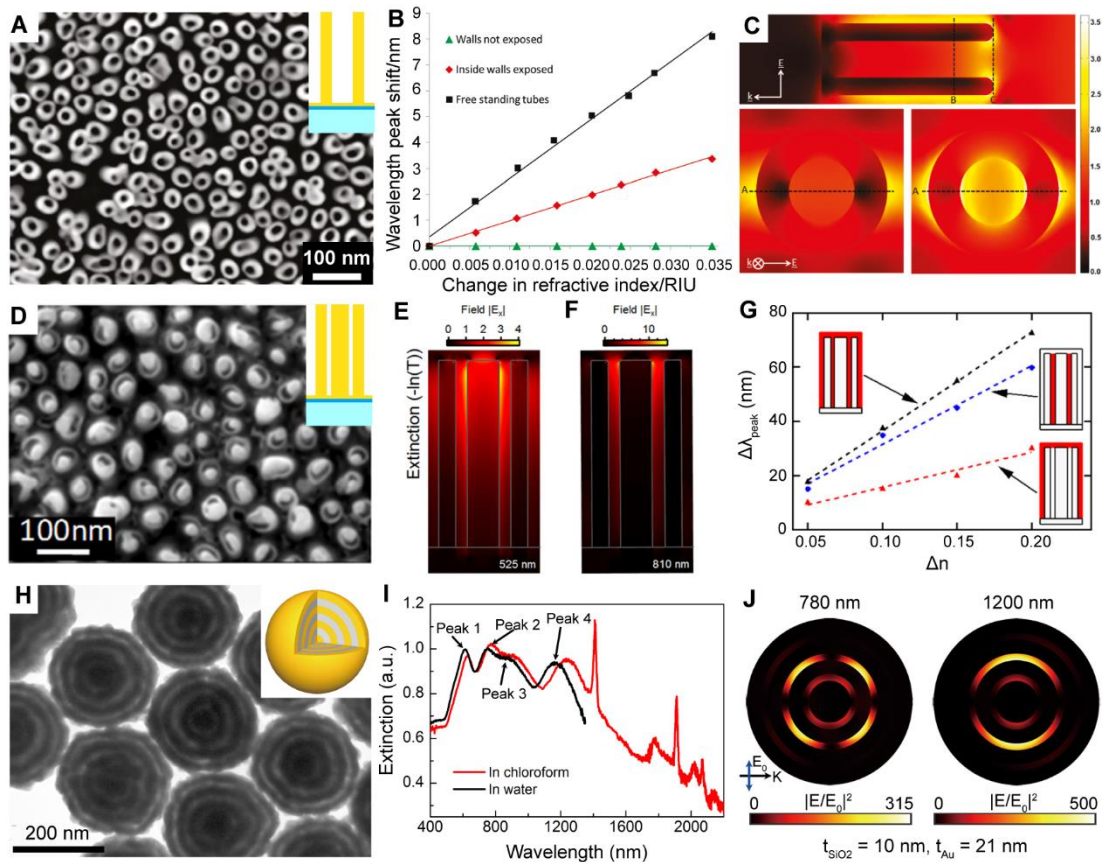


**Figure 5.** Optical sensing based on alternative plasmonic metamaterials. (A) SEM image of a gold nanotube array. (B) Sensitivity of the spectral position of the extinction peak to changes in the surrounding RI when different walls of the nanotubes are exposed to analyte. (C) The distributions of the electric field norm for the free-standing gold nanotube arrays at the wavelength of maximum extinction. (A–C) Reproduced with permission from ref 40. Copyright 2010 American Chemical Society. (D) SEM image of a gold coaxial rod-tube array. (E, F) Cross-section of the  $|E_x|$  component of the field for 525 and 810 nm excitation wavelengths. (G) The bulk RI sensitivity of the coaxial structure for different walls exposed for the lower energy resonance. (D–G) Reproduced with permission from Ref. 60. Copyright 2013 American Institute of Physics. (H) TEM image of metaparticles with three pairs of  $\text{SiO}_2/\text{Au}$  shells. (I) Extinction spectra of the metaparticles dispersed in water and chloroform. (J) Electric field distributions in the metaparticle at the wavelengths of 780 and 1200 nm, respectively. (H–J) Reproduced with permission from ref 61. Copyright 2018 Wiley.

## 7. NANOCHEMISTRY AND SENSING WITH ELECTRICALLY-DRIVEN NANOROD METAMATERIALS

In all kinds of plasmonic sensors, an external light source is needed for the optical excitation of plasmonic modes.<sup>17</sup> The use of lasers, fibres, lenses, mirrors, prisms or objectives which are often required, making it difficult to realize plasmonic sensors with miniaturized sizes and low operating powers. Recent realization of the electrically-driven plasmonic nanorod metamaterial provides the opportunity to use an electron tunneling effect for the excitation of surface plasmons and hot-electrons,<sup>26</sup> opening a way to realize a new kind of hot-electron-activated nanoreactors, as well as highly compact and sensitive plasmonic sensors.

### 7.1. Plasmon Excitation based on Inelastic Electron Tunneling

When an electric bias is applied across a metal-insulator-metal junction with nanometer-scale insulator thickness, electrons can tunnel through the insulator layer due to quantum mechanical tunneling. The resulting current depends exponentially on the gap size so that even an atomic-level variation in the gap distance can produce a measurable change in the tunneling current. At the same time, broad-band light emission from a metal-insulator-metal tunnel junction has been observed,<sup>62</sup> which is due to the radiative decay of surface plasmon modes in the junction excited by inelastically tunneled electrons. The electron-to-photon conversion efficiency has been greatly improved by combining tunnel junctions with optical antennas,<sup>63-66</sup> reaching a value around 2% by optimizing local density of optical states and radiation efficiency of the junctions.<sup>66</sup> The electron tunneling effect provides an attractive approach for the direct electrical excitation of plasmons in metallic nanostructures with high compactness and low operation power.

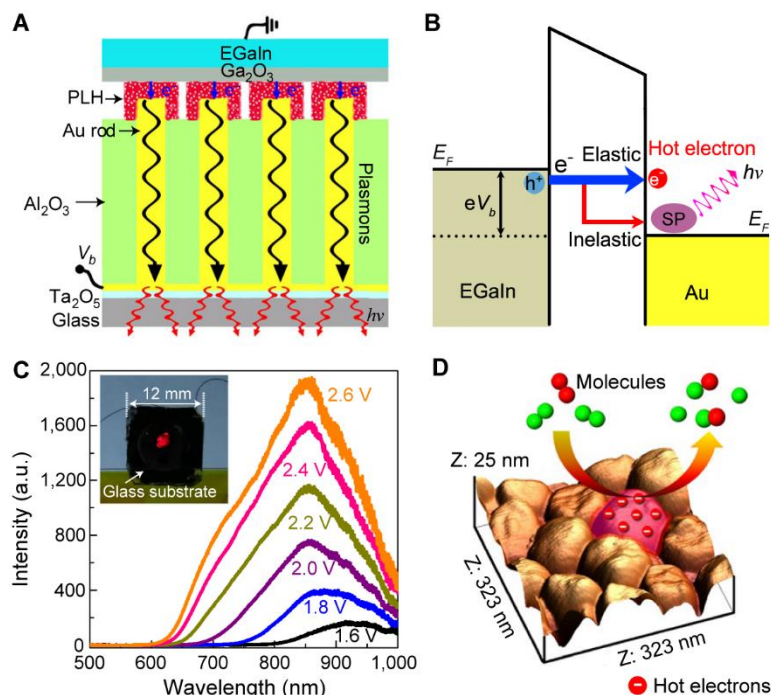


**Figure 6.** Electrically-driven plasmonic nanorod metamaterials. (A) Schematic diagram of the device based on metal-polymer-metal tunnel junctions. (B) Inelastic and elastic electron tunneling in plasmonic tunnel junctions for the excitation of plasmons and generation of hot electrons, respectively. (C) Emission spectra of an electrically-driven gold nanorod array as a function of the applied bias. Inset, photograph of the nanorod metamaterial under a 2.5 V bias. (D) Schematic of hot-electron-activated chemical reactions on the tips of nanorods in plasmonic tunnel junctions. Reproduced with permission from ref 26. Copyright 2018 Nature Publishing Group.

In a plasmonic nanorod metamaterial, each nanorod forms a tunnel junction and the density of optical states provided by the metamaterial facilitates shaping of the emission spectrum.<sup>26</sup> The size of the nanorods also facilitates tunneling process due to the relaxation of the electron momentum conservation via scattering on the tips and rims.<sup>20</sup> To construct tunnel junctions, a monolayer of poly-L-histidine (PLH) was self-assembled onto the gold nanorod tips to work as the tunnel barrier, and a droplet of eutectic gallium indium (EGaIn) was used as the top electrode

(Figure 6A). When a bias is applied, the inelastic tunneling of electrons excites the modes of the metamaterial (Figure 6B), resulting in an obvious light emission of a distinctly red color observed from the substrate side due to the radiative decay of the plasmons (Figure 6C). With the increase of applied bias, the emission intensity increased gradually, together with a blue-shift of the emission peak. The emission spectrum is defined by the product of the bias-dependent spectral density of the tunneling current, local density of electromagnetic states in the junction region and the near-to-far field conversion efficiency of the metamaterial. As the result of the high-density of tunnel junctions arrayed in these macroscopic devices ( $\sim 10^{10} \text{ cm}^{-2}$ ), the emission is visible to the naked eye making signal detection trivial for sensing applications.

## 7.2. Hot-electron Chemistry and Sensing

During the tunneling process, the majority of electrons ( $\sim 99.9\%$ , considering an estimated inelastic tunneling efficiency of  $\sim 0.1\%$ ) tunnel elastically in the electrically-driven nanorod metamaterials,<sup>26</sup> appearing as energetic hot electrons<sup>11</sup> in the nanorod tips (Figure 6B). The highly efficient and confined hot-electron generation makes the tunnel junctions highly reactive and opens up opportunities for the precise activation of chemical reactions in the junctions (Figure 6D). In this case, the electrically-driven nanorod metamaterial can be used as an array of high-density nanoreactors for in situ studies of chemical transformation of molecules in the junctions, which is attractive for chemical and pharmaceutical industries.

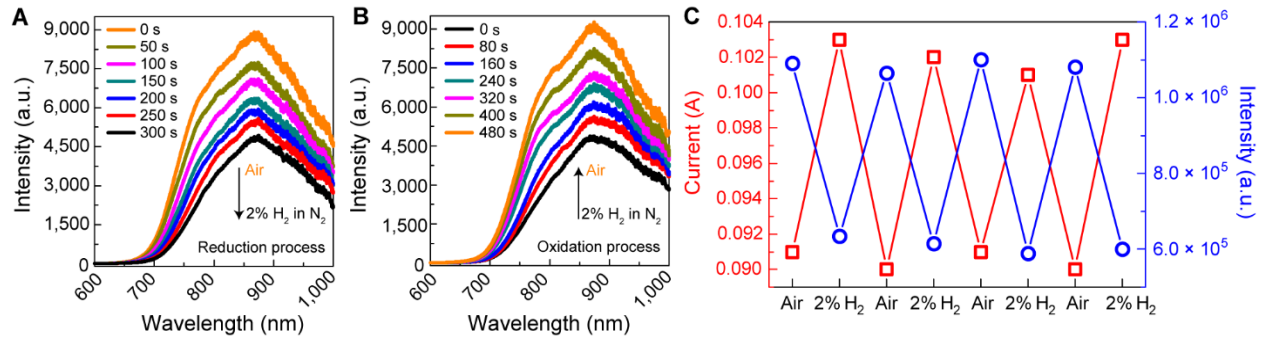


**Figure 7.** Gas sensing based on chemical reactions in the plasmonic tunnel junctions. (A, B) The evolution of the emission spectra of an electrically-driven metamaterial ( $V_b = 2.5$  V) when the cell atmosphere was switched (A) from air to 2% H<sub>2</sub> and (B) from 2% H<sub>2</sub> to air. (C) Tunneling current (red) and emission power (blue) measured when the cell atmosphere was cycled between air and 2% H<sub>2</sub>. Reproduced with permission from Ref. 26. Copyright 2018 Nature Publishing Group.

The highly-confined electron tunneling process is extremely sensitive to any changes in the junction, thus, the chemical transformations in electrically-driven plasmonic nanorod metamaterials can be detected with atomic-level sensitivity by observing the light emission from the tunnel junction or tunneling current changes.

This was demonstrated for both hydrogen and oxygen sensing based on electrically-driven metamaterials.<sup>26</sup> Under a bias of 2.5 V, when 2% H<sub>2</sub> was introduced to replace air in the gas cell, the light emission intensity decreases gradually to approximately one half of the original value (Figure 7A). When air containing oxygen was subsequently introduced into the gas cell, the emission intensity increased gradually, returning to the initial value (Figure 7B). The sensing mechanism is hot electron-mediated oxidation and reduction of the tunnel junctions. The reactions in the tunnel junctions caused changes both in the light emission and tunneling current (Figure 7C). However, the changes in the emission intensity are about five times higher than that of the tunneling current (50% versus 10%), indicating the high sensitivity of optical detection for

tunneling-based sensors. By choosing an appropriate material for the functionalization of tunnel junctions, they can be designed to transduce a variety of chemical and physical stimuli. The reactions can also be stimulated in the junctions without the electric bias, under the illumination of the nanorod metamaterial which also generates hot-electrons, albeit with broad energy spectrum, as opposed to monochromatic in the elastic tunneling process, and the rate depending on the illumination intensity.<sup>11</sup>

Feedback generated by the chemical reactions in the junction influences the tunneling current and the emission intensity. Therefore, promoting and stopping the reactions with the choice of the gas environment, lead to the realization of the nonvolatile and multilevel memory device using reactive tunnel junctions.<sup>67</sup> Therefore, the electrically-driven-metamaterial platform can also function as an optoelectronic memristor. The information can be written into the junctions both electrically or optically via the hot-electron-mediated chemical reactions and read out by measuring the resistance or light emission, respectively. It has the potential to become important building block of memories, logic units, or artificial synapses in optoelectronic or neuromorphic computing systems.

## 8. CONCLUSION AND OUTLOOK

We have reviewed our recent progress in the sensing and nanochemistry applications of plasmonic nanorod metamaterials and other related platforms. As a result of the strong plasmonic interaction in the nanorod array, the significant flexibility in material and structural design as well as the discontinuous porous nanotexture, plasmonic nanorod metamaterials provide a versatile platform for the development of multimodal optical sensors with excellent performance. The enhanced nonlinear optical effects in the metamaterials also stem from the high sensitivity to the RI changes

with the illumination intensity.<sup>6,29,30</sup> Integration of magneto-optical materials in the nanorod metamaterial allows optical sensing of magnetic fields and applications in non-reciprocal photonic devices.<sup>51</sup> The use of hot-electron effects additionally provides new sensing opportunities due to chemical transformation in the nanoscale tunnel junctions. In parallel, the tunnel junctions act as nanoscale chemical reactors capable to catalyze reaction pathways which would be impossible without the hot-electron contribution.

Future improvements of the presented sensing and nanochemistry platforms may include optimization of the plasmonic material quality via hot-electron mediated growth method<sup>68</sup> instead of electrochemical deposition to reduce the losses and to improve sensing performance. The extension of the electrically-driven metamaterials for the detection of liquid analytes can also be envisaged. Plasmonic sensors based on the versatile nanorod metamaterial platform, benefitting from the low cost, geometrical flexibility and scalability afforded by the templated electrodeposition method, are becoming truly attractive for applications in fundamental research and a plethora of industries such as environmental monitoring, food safety, and healthcare. Multiplexing several different sensing and nanochemistry functionalities in one plasmonic metamaterial platform provides a test-bed for inducing, monitoring and exploring chemical events in real time, which can provide valuable information on reaction pathways, mechanism and rates.

## AUTHOR INFORMATION

### **Corresponding Author**

\*E-mail: [nanopan@zju.edu.cn](mailto:nanopan@zju.edu.cn); [a.zayats@kcl.ac.uk](mailto:a.zayats@kcl.ac.uk).

### **Author Contributions**

The manuscript was written through contributions of all authors. All authors have given approval to the final version of the manuscript.

## Notes

The authors declare no competing financial interests.

## Biographies

**Pan Wang** is a Professor at the State Key Laboratory of Modern Optical Instrumentation, College of Optical Science and Engineering, Zhejiang University, China.

**Mazhar E. Nasir** is a Research Associate at the Department of Physics, King's College London.

**Alexey V. Krasavin** is a Research Associate at the Department of Physics, King's College London.

**Wayne Dickson** is a Senior Lecturer at the Department of Physics, King's College London.

**Yunlu Jiang** is a Ph. D. student at the Department of Physics, King's College London.

**Anatoly V. Zayats** is a Chair in Experimental Physics and the Head of the Photonics and Nanotechnology Group at the Department of Physics, King's College London, where he also leads Nano-optics and Near-field Spectroscopy Laboratory. He is also a Co-Director of the London Centre for Nanotechnology and the London Institute of Advanced Light Technologies. He is a Fellow of the Institute of Physics, the Optical Society of America, SPIE and the Royal Society of Chemistry.

## ACKNOWLEDGMENT

This work has been funded in part by the Engineering and Physical Sciences Research Council (UK) and the European Research Council iPLASMM project (321268).

## REFERENCES

- (1) Zayats, A. V., Smolyaninov, I. I., Maradudin, A. A. Nano-optics of surface plasmon polaritons. *Phys. Rep.* **2005**, *408*, 2005, 131-314.
- (2) Schuller, J. A.; Barnard, E. S.; Cai, W. S.; Jun, Y. C.; White, J. S.; Brongersma, M. L. Plasmonics for Extreme Light Concentration and Manipulation. *Nat. Mater.* **2010**, *9*, 193–204.
- (3) Lal, S.; Link, S.; Halas, N. J. Nano-Optics from Sensing to Waveguiding. *Nat. Photon.* **2007**, *1*, 641–648.
- (4) Homola, J. Surface Plasmon Resonance Sensors for Detection of Chemical and Biological Species. *Chem. Rev.* **2008**, *108*, 462–493.
- (5) Nam, J. -M.; Oh, J. -W.; Lee, H.; Suh, Y. D. Plasmonic Nanogap-Enhanced Raman Scattering with Nanoparticles. *Acc. Chem. Res.* **2016**, *49*, 2746–2755.
- (6) Kauranen, M.; Zayats, A. V. Nonlinear Plasmonics. *Nature Photon.* **2012**, *6*, 737–748.
- (7) Tsai, K.-T.; Wurtz, G. A.; Chu, J.-Y.; Cheng, T.-Y.; Wang, H.-H.; Krasavin, A. V.; He, J.-H.; Wells, B. M.; Podolskiy, V. A.; Wang, J.-K.; Wang, Y.-L.; Zayats, A. V. Looking into “Meta-atoms” of Plasmonic Nanowire Metamaterial. *Nano Lett.* **2014**, *14*, 4971–4976.
- (8) Chikkaraddy, R.; de Nijs, B.; Benz, F.; Barrow, S. J.; Scherman, O. A.; Rosta, E.; Demetriadou, A.; Fox, P.; Hess, O.; Baumberg, J. J. Single-Molecule Strong Coupling at Room Temperature in Plasmonic Nanocavities. *Nature* **2016**, *535*, 127–130.

- (9) Mubeen, S.; Lee, J.; Singh, N.; Krämer, S.; Stucky, G. D.; Moskovits, M. An Autonomous Photosynthetic Device in which All Charge Carriers Derive from Surface Plasmons. *Nature Nanotechnol.* **2013**, *8*, 247–251.
- (10) Knight, M. W.; Sobhani, H.; Nordlander, P.; Halas, N. J. Photodetection with Active Optical Antennas. *Science* **2011**, *332*, 702–704.
- (11) Brongersma, M. L.; Halas, N. J.; Nordlander, P. Plasmon-Induced Hot Carrier Science and Technology. *Nat. Nanotechnol.* **2015**, *10*, 25–34.
- (12) Liu, Y. M.; Zhang, X. Metamaterials: A New Frontier of Science and Technology. *Chem. Soc. Rev.* **2011**, *40*, 2494–2507.
- (13) Ernst, S.; Gordon II, J. G. Surface Plasmons as a Probe of the Electrochemical Interface. *Surf. Sci.* **1980**, *101*, 499–506.
- (14) Nylander, C.; Liedberg, B.; Lind, T. Gas Detection by Means of Surface Plasmon Resonance. *Sens. Actuators* **1982**, *3*, 79–88.
- (15) Stewart, M. E.; Anderton, C. R.; Thompson, L. B.; Maria, J.; Gray, S. K.; Rogers, J. A.; Nuzzo, R. G. Nanostructured Plasmonic Sensors. *Chem. Rev.* **2008**, *108*, 494–521.
- (16) Nie, S. M.; Emory, S. R. Probing Single Molecules and Single Nanoparticles by Surface-Enhanced Raman Scattering. *Science* **1997**, *275*, 1102–1106.
- (17) Prabowo, B. A.; Purwidyantri, A.; Liu, K. -C. Surface Plasmon Resonance Optical Sensor: A Review on Light Source Technology. *Biosensor* **2018**, *8*, 80–106.
- (18) Anker, J. N.; Hall, W. P.; Lyandres, O.; Shah, N. C.; Zhao, J.; van Duyne R. P. Biosensing with Plasmonic Nanosensors. *Nat. Mater.* **2008**, *7*, 442–453.

- (19) Chen, H. J.; Shao, L.; Woo, K. C.; Ming, T.; Lin, H. -Q.; Wang, J. F. Shape-Dependent Refractive Index Sensitivities of Gold Nanocrystals with the Same Plasmon Resonance Wavelength. *J. Phys. Chem. C* **2009**, *113*, 17691–17697.
- (20) Grajower, M.; Levy, U.; Khurgin, J. B. The Role of Surface Roughness in Plasmonic-Assisted Internal Photoemission Schottky Photodetectors. *ACS Photon.* **2018**, *5*, 4030–4036.
- (21) Salmon-Gamboa, J. U.; Romero-Gomez, M.; Roth, D. J.; Barber, M. J.; Wang, P.; Gairclough, S. M.; Nasir, M. E.; Krasavin, A. V.; Dickson, W.; Zayats, A. V. Optimizing Hot Carrier Effects in Pt-Decorated Plasmonic Heterostructures. *Faraday Discuss.* **2019**, *214*, 387–397.
- (22) Lu, X. M.; Rycenga, M.; Skrabalak, S. E.; Wiley, B.; Xia, Y. N. Chemical Synthesis of Novel Plasmonic Nanoparticles. *Annu. Rev. Phys. Chem.* **2009**, *60*, 167–192.
- (23) Martin, C. R. Nanomaterials: A Membrane-Based Synthetic Approach. *Science* **1994**, *266*, 1961–1966.
- (24) Sander, M. S.; Tan, L.-S. Nanoparticle Arrays on Surfaces Fabricated Using Anodic Alumina Films as Templates. *Adv. Funct. Mater.* **2003**, *13*, 393–397.
- (25) Evans, P.; Hendren, W. R.; Atkinson, R.; Wurtz, G. A.; Dickson, W.; Zayats, A. V.; Pollard R. J. Growth and Properties of Gold and Nickel Nanorods in Thin Film Alumina. *Nanotechnology* **2006**, *17*, 5746–5753.
- (26) Wang, P.; Krasavin, A. V.; Nasir, M. E.; Dickson, W.; Zayats, A. V. Reactive Tunnel Junctions in Electrically Driven Plasmonic Nanorod Metamaterials. *Nat. Nanotechnol.* **2018**, *13*, 159–164.
- (27) Yao, J.; Liu, Z. W.; Liu, Y. M.; Wang, Y.; Sun, C.; Bartal, G.; Stacy, A. M.; Zhang, X. Optical Negative Refraction in Bulk Metamaterials of Nanowires. *Science* **2008**, *321*, 930.

- (28) Vasilantonakis, N.; Nasir, M. E.; Dickson, W.; Wurtz, G. A.; Zayats, A. V. Bulk Plasmon-Polaritons in Hyperbolic Nanorod Metamaterial Waveguides. *Laser Photonics. Rev.* **2015**, *9*, 345–353.
- (29) Wurtz, G. A.; Pollard, R.; Hendren, W.; Wiederrecht, G. P.; Gosztola, D. J.; Podolskiy, V. A.; Zayats, A. V. Designed Ultrafast Optical Nonlinearity in a Plasmonic Nanorod Metamaterial Enhanced by Nonlocality. *Nat. Nanotechnol.* **2011**, *6*, 107–111.
- (30) Nicholls, L. H.; Rodríguez-Fortuño, F. J.; Nasir, M. E.; Córdova-Castro, R. M.; Olover, N.; Wurtz, G. A.; Zayats, A. V. Ultrafast Synthesis and Switching of Light Polarization in Nonlinear Anisotropic Metamaterials. *Nat. Photon.* **2017**, *11*, 628–633.
- (31) Roth, D. J.; Krasavin, A. V.; Wade, A.; Dickson, W.; Murphy, A.; Kéna-Cohen, S.; Pollard, R.; Wurtz, G. A.; Richards, D.; Maier, S. A.; Zayats, A. V. Förster Resonance Energy Transfer inside Hyperbolic Metamaterials. *ACS Photon.* **2017**, *4*, 2513–2521.
- (32) Elser, J.; Wangberg, R.; Podolskiy, V. A.; Narimanov, E. E. Nanowire Metamaterials with Extreme Optical Anisotropy. *Appl. Phys. Lett.* **2006**, *89*, 261102.
- (33) Pollard, R. J.; Murphy, A.; Hendren, W. R.; Evans, P. R.; Atkinson, R.; Wurtz, G. A.; Zayats, A. V.; Podolskiy, V. A. Optical Nonlocalities and Additional Waves in Epsilon-Near-Zero Metamaterials. *Phys Rev. Lett.* **2009**, *102*, 127405.
- (34) Jain, P. K.; Eustis, S.; El-Sayed, M. A. Plasmon Coupling in Nanorod Assemblies: Optical Absorption, Discrete Dipole Approximation Simulation, and Exciton-Coupling Model. *J. Phys. Chem. B* **2006**, *110*, 18243–18253.
- (35) Wurtz, G. A.; Dickson, W.; O'Connor, D.; Atkinson, R.; Hendren, W.; Evans, P.; Pollard, R.; Zayats, A. V. Guided Plasmonic Modes in Nanorod Assemblies: Strong Electromagnetic Coupling Regime. *Opt. Express* **2008**, *16*, 7460-7470.

- (36) Doherty, M. D.; Murphy, A.; Pollard, R. J.; Dawson, P. Surface-Enhanced Raman Scattering from Metallic Nanostructures: Bridging the Gap between the Near-Field and Far-Field Responses. *Phys. Rev. X* **2013**, *3*, 11001.
- (37) Kabashin, A. V.; Evans, P.; Pastkovsky, S.; Hendren, W.; Wurtz, G. A.; Atkinson, R.; Pollard, R.; Podolskiy, V. A.; Zayats, A. V. Plasmonic Nanorod Metamaterials for Biosensing. *Nat. Mater.* **2009**, *8*, 867–871.
- (38) Nasir, M. E., Peruch, S., Vasilantonakis, N., Wardley, W. P., Dickson, W., Wurtz, G. A. & Zayats, A. V. Tuning the Effective Plasma Frequency of Nanorod Metamaterials from Visible to Telecom Wavelengths. *Appl. Phys. Lett.* **2015**, *107*, 121110.
- (39) Vasilantonakis, N.; Wurtz, G. A.; Podolskiy, V. A.; Zayats, A. V. Refractive Index Sensing with Hyperbolic Metamaterials: Strategies for Biosensing and Nonlinearity Enhancement. *Opt. Express* **2015**, *23*, 14329–14343.
- (40) McPhillips, J.; Murphy, A.; Jonsson, M. P.; Hendren, W. R.; Atkinson, R.; Höök, F.; Zayats, A. V.; Pollard, R. J. High-Performance Biosensing Using Arrays of Plasmonic Nanotubes. *ACS Nano* **2010**, *4*, 2210–2216.
- (41) Love, J. C.; Estroff, L. A.; Kriebel, J. K.; Nuzzo, R. G.; Whitesides, G. M. Self-Assembled Monolayers of Thiolates on Metals as a Form of Nanotechnology. *Chem. Rev.* **2005**, *105*, 1103–1169.
- (42) Evans, P. R., Wurtz, G. A., O'Connor, D., Atkinson, R., Hendren, W., Dickson, W., Pollard, R. J., Zayats, A. V., Plasmonic Core/shell Nanorod Arrays: Sub-atto-liter Controlled Geometry and Tunable Optical Properties, *J. Phys. Chem. C* **2007**, *111*, 12522–12527.

- (43) Zhang, R.; Zhang, Y.; Dong, Z. C.; Jiang, S.; Zhang, C.; Chen, L. G.; Zhang, L.; Liao, Y.; Aizpurua, J.; Luo, Y.; Yang, J. L.; Hou, J. G. Chemical Mapping of a Single Molecule by Plasmon-Enhanced Raman Scattering. *Nature* **2013**, 498, 82–86.
- (44) Lee, S. J.; Guan, Z. Q.; Xu, H. X.; Moskovits, M. Surface-Enhanced Raman Spectroscopy and Nanogeometry: The Plasmonic Origin of SERS. *J. Phys. Chem. C* **2007**, 111, 17985–17988.
- (45) Doherty, M. D.; Murphy, A.; McPhillips, J.; Pollard, R. J.; Dawson, P. Wavelength Dependence of Raman Enhancement from Gold Nanorod Arrays: Quantitative Experiment and Modeling of a Hot Spot Dominated System. *J. Phys. Chem. C* **2010**, 114, 19913–19919.
- (46) Esteban, R.; Borisov, A. G.; Nordlander, P.; Aizpurua, J. Bridging Quantum and Classical Plasmonics with a Quantum-Corrected Model. *Nat. Commun.* **2012**, 3, 825.
- (47) Cheng, Z. -Q.; Nan, F.; Yang, D. -J.; Zhong, Y. -T.; Ma, L.; Hao, Z. -H.; Zhou, L.; Wang, Q. -Q. Plasmonic Nanorod Arrays of a Two-Segment Dimer and a Coaxial Cable with 1 nm Gap for Large Field Confinement and Enhancement. *Nanoscale* **2015**, 7, 1463–1470.
- (48) Córdova-Castro, R. M.; Krasavin, A. V.; Nasir, M. E.; Zayats, A. V.; Dickson, W. Nanocone-based Plasmonic Metamaterials. *Nanotechnology* **2019**, 30, 055301.
- (49) Nasir, M. E.; Dickson W.; Wurtz, G. A.; Wardley, W. P.; Zayats, A. V. Hydrogen Detected by the Naked Eye: Optical Hydrogen Gas Sensors Based on Core/Shell Plasmonic Nanorod Metamaterials. *Adv. Mater.* **2014**, 26, 3532–3537.
- (50) Yakovlev, V. V.; Dickson, W.; Murphy, A.; McPhillips, J.; Pollard, R. J.; Podolskiy, V. A.; Zayats, A. V. Ultrasensitive Non-Resonant Detection of Ultrasound with Plasmonic Metamaterials. *Adv. Mater.* **2013**, 25, 2351–2356.

- (51) Fan, B.; Nasir, M. E.; Nicholls, L. H.; Zayats, A. V.; Podolskiy, V. A. Magneto-Optical Metamaterials: Nonreciprocal Transmission and Faraday Effect Enhancement. *Adv. Optical Mater.* **2019**, *7*, 1801420.
- (52) Buttner, W. J.; Post, M. B.; Burgess, R.; Rivkin, C. An Overview of Hydrogen Safety Sensors and Requirements. *Int. J. Hydrog. Energy* **2011**, *36*, 2462–2470.
- (53) Hübert, T.; Boon-Brett, L.; Palmisano, V.; Bader, M. A. Developments in Gas Sensor Technology for Hydrogen Safety. *Int. J. Hydrog. Energy* **2014**, *39*, 20474–20483.
- (54) Wang, Z. J.; Li, Z. Y.; Jiang, T. T.; Xu, X. R.; Wang, C. Ultrasensitive Hydrogen Sensor Based on Pd<sup>0</sup>-Loaded SnO<sub>2</sub> Electrospun Nanofibers at Room Temperature. *ACS Appl. Mater. Interfaces* **2013**, *5*, 2013–2021.
- (55) Wadell, C.; Syrenova, S.; Langhammer, C. Plasmonic Hydrogen Sensing with Nanostructured Metal Hydrides. *ACS Nano* **2014**, *8*, 11925–11940.
- (56) Murphy, A.; McPhillips, J.; Hendren, W.; McClatchey, C.; Atkinson, R.; Wurtz, G.; Zayats, A. V.; Pollard, R. J. The Controlled Fabrication and Geometry Tunable Optics of Gold Nanotube Arrays. *Nanotechnology* **2011**, *22*, 045705.
- (57) Tadigadapa, S.; Mateti, K. Piezoelectric MEMS Sensors: State-of-the-Art and Perspectives. *Meas. Sci. Technol.* **2009**, *20*, 092001.
- (58) Ling, T.; Chen, S.-L.; Guo, L. J. Fabrication and Characterization of High Q Polymer Micro-Ring Resonator and Its Application as a Sensitive Ultrasonic Detector. *Opt. Express* **2011**, *19*, 861–869.
- (59) Hendren, W. R.; Murphy, A.; Evans, P.; O'Connor, D.; Wurtz, G. A.; Zayats, A. V.; Atkinson, R.; Pollard, R. J. Fabrication and Optical Properties of Gold Nanotube Arrays. *J. Phys. Condens. Matter* **2008**, *20*, 362203.

- (60) Murphy, A.; Sonnefraud, Y.; Krasavin, A. V.; Ginzburg, P.; Morgan, F.; McPhillips, J.; Wurtz, G. A.; Maier, S. A.; Zayats, A. V.; Pollard, R. J. Fabrication and Optical Properties of Large-Scale Arrays of Gold Nanocavities based on Rod-in-a-Tube Coaxials. *Appl. Phys. Lett.* **2013**, *102*, 103103.
- (61) Wang, P.; Krasavin, A. V.; Viscomi, F. N.; Adawi, A. M.; Bouillard, J. -S. G.; Zhang, L.; Roth, D. J.; Tong, L. M.; Zayats, A. V. Metaparticles: Dressing Nano-Objects with a Hyperbolic Coating. *Laser Photonics Rev.* **2018**, *12*, 1800179.
- (62) Lambe, J.; McCarthy, S. L. Light Emission from Inelastic Electron Tunneling. *Phys. Rev. Lett.* **1976**, *37*, 923–925.
- (63) Kern, J.; Kulloock, R.; Prangma, J.; Emmerling, M.; Kamp, M.; Hecht, B. Electrically Driven Optical Antennas. *Nat. Photon.* **2015**, *9*, 582–586.
- (64) Parzefall, M.; Bharadwaj, P.; Jain, A.; Taniguchi, T.; Watanabe, K.; Novotny, L. Antenna-Coupled Photon Emission from Hexagonal Boron Nitride Tunnel Junctions. *Nat. Nanotechnol.* **2015**, *10*, 1058–1063.
- (65) Du, W.; Wang, T.; Chu, H. -S.; Nijhuis, C. A. Highly Efficient On-Chip Direct Electronic-Plasmonic Transducers. *Nat. Photon.* **2017**, *11*, 623–627.
- (66) Qian, H. L.; Hsu, S. -W.; Gurunatha, K.; Riley, C. T.; Zhao, J.; Lu, D.; Tao, A. R.; Liu, Z. W. Efficient Light Generation from Enhanced Inelastic Electron Tunnelling. *Nat. Photon.* **2018**, *12*, 485–488.
- (67) Wang, P., Nasir, M. E., Krasavin, A. V., Dickson, W., Zayats, A. V., Multilevel nonvolatile optoelectronic memory based on memristive plasmonic tunnel junctions. *arXiv.* **2018**, 1811.03347.

- (68) Zhai, Y. M.; DuChene, J. S.; Wang, Y. -C.; Qiu, J. J.; Johnston-Peck, A. C.; You, B.; Guo, W. X.; DiCiaccio, B.; Qian, K.; Zhao, E. W.; Ooi, F.; Hu, D. H.; Su, D.; Stach, E. A.; Zhu, Z. H.; Wei, W. D. Polyvinylpyrrolidone-Induced Anisotropic Growth of Gold Nanoprisms in Plasmon-Driven Synthesis. *Nat. Mater.* **2016**, *15*, 889–895.